RESEARCH BRIEF

PD-1 Blockade in Solid Tumors with Defects in Polymerase Epsilon

Benoit Rousseau[1], Ivan Bieche[2,3], Eric Pasmant[3,4], Nadim Hamzaoui[3,4], Nicolas Leulliot[5], Lucas Michon[6], Aurelien de Reynies[7], Valerie Attignon[8], Michael B. Foote[1], Julien Masliah-Planchon[2], Magali Svrcek[9,10], Romain Cohen[10,11], Victor Simmet[12], Paule Augereau[12], David Malka[13], Antoine Hollebecque[13], Damien Pouessel[14], Carlos Gomez-Roca[14], Rosine Guimbaud[15], Amandine Bruyas[16], Marielle Guillet[17], Jean-Jacques Grob[18], Muriel Duluc[18], Sophie Cousin[19], Christelle de la Fouchardiere[20], Aude Flechon[20], Frederic Rolland[21], Sandrine Hiret[21], Esma Saada-Bouzid[22], Olivier Bouche[23], Thierry Andre[11], Diane Pannier[24], Farid El Hajbi[24], Stephane Oudard[25], Christophe Tournigand[26], Jean-Charles Soria[13], Stephane Champiat[13], Drew G. Gerber[1], Dennis Stephens[1], Michelle F. Lamendola-Essel[1], Steven B. Maron[1], Bill H. Diplas[27], Guillem Argiles[1], Asha R. Krishnan[1], Severine Tabone-Eglinger[28], Anthony Ferrari[29], Neil H. Segal[1], Andrea Cercek[1], Natalie Hoog-Labouret[30], Frederic Legrand[30], Clotilde Simon[31], Assia Lamrani-Ghaouti[31], Luis A. Diaz Jr[1], Pierre Saintigny[6,20], Sylvie Chevret[32], and Aurelien Marabelle[13,33,34]

ABSTRACT Missense mutations in the polymerase epsilon (*POLE*) gene have been reported to generate proofreading defects resulting in an ultramutated genome and to sensitize tumors to checkpoint blockade immunotherapy. However, many *POLE*-mutated tumors do not respond to such treatment. To better understand the link between *POLE* mutation variants and response to immunotherapy, we prospectively assessed the efficacy of nivolumab in a multicenter clinical trial in patients bearing advanced mismatch repair–proficient *POLE*-mutated solid tumors. We found that only tumors harboring selective *POLE* pathogenic mutations in the DNA binding or catalytic site of the exonuclease domain presented high mutational burden with a specific single-base substitution signature, high T-cell infiltrates, and a high response rate to anti–PD-1 monotherapy. This study illustrates how specific DNA repair defects sensitize to immunotherapy. POLE proofreading deficiency represents a novel agnostic biomarker for response to PD-1 checkpoint blockade therapy.

SIGNIFICANCE: POLE proofreading deficiency leads to high tumor mutational burden with high tumor-infiltrating lymphocytes and predicts anti–PD-1 efficacy in mismatch repair–proficient tumors. Conversely, tumors harboring *POLE* mutations not affecting proofreading derived no benefit from PD-1 blockade. POLE proofreading deficiency is a new tissue-agnostic biomarker for cancer immunotherapy.

See related video: https://vimeo.com/720727355

[1]Department of Medicine, Memorial Sloan Kettering Cancer Center, New York, New York. [2]Department of Genetics, Institut Curie, Paris, France. [3]Institut Cochin, INSERM U1016, CNRS UMR8104, Université de Paris, CARPEM, Paris, France. [4]Fédération de Génétique et Médecine Génomique, Hôpital Cochin, AP-HP Centre-Université de Paris, Paris, France. [5]Cibles Thérapeutiques et Conception de Médicaments, CNRS UMR8015, Université de Paris, UFR de Pharmacie de Paris, Paris, France. [6]Univ Lyon, Université Claude Bernard Lyon 1, INSERM 1052, CNRS 5286, Centre Léon Bérard, Centre de Recherche en Cancérologie de Lyon, Lyon, France. [7]Université de Paris, Centre de Recherche des Cordeliers, UMRS1138, AP-HP, SeqOIA-IT, Paris, France. [8]Platform of Cancer Genomics, Centre Léon Bérard, Lyon, France. [9]Pathology Department, Saint-Antoine Hospital, Paris, France. [10]Sorbonne Université, INSERM, Unité Mixte de Recherche Scientifique 938 and SIRIC CURAMUS, Centre de Recherche Saint-Antoine, Equipe Instabilité des Microsatellites et Cancer, Equipe labellisée par la Ligue Nationale contre le Cancer, Paris, France. [11]Medical Oncology Department, Hôpital Saint-Antoine, Paris, France. [12]Department of Medical Oncology, Institut de Cancérologie de l'Ouest (ICO), Angers, France. [13]Département d'Innovation Thérapeutique et d'Essais Précoces (DITEP), Gustave Roussy, Université Paris Saclay, Villejuif, France. [14]Department of Medical Oncology, Institut Claudius Regaud/IUCT Oncopole, Toulouse, France. [15]Medical Oncology, CHU de Toulouse, Toulouse, France. [16]Department of Medical Oncology, Hôpital de la Croix-Rousse, Lyon, France. [17]Department of Gastroenterology and Digestive Oncology, Hôpital de la Croix-Rousse, Lyon, France. [18]Dermatology and Oncology, Hôpital de la Timone, Marseille, France. [19]Oncology, Institut Bergonie, Bordeaux, France. [20]Department of Medical Oncology, Centre Léon Bérard, Lyon, France. [21]Department of Medical Oncology, ICO Institut de Cancérologie de l'Ouest René Gaudducheau, Saint-Herblain, France. [22]Medical Oncology, Centre Anticancer Antoine Lacassagne, Nice, France. [23]Gastroenterology and Digestive Oncology, CHU de Reims, Hôpital Robert Debré, Reims, France. [24]Oncology, Centre Oscar Lambret, Lille, France. [25]Oncology, Hôpital Europeen Georges Pompidou, AP-HP, Paris, France. [26]Oncology, Hôpital Henri Mondor, AP-HP, Creteil, France. [27]Department of Radiation Oncology, Memorial Sloan Kettering Cancer Center, New York, New York. [28]Biobank, Centre Léon Bérard, Lyon, France. [29]Platform of Bioinformatics Gilles Thomas-Synergie Lyon Cancer, Centre Léon Bérard, Lyon, France. [30]Research and Innovation, Institut National du Cancer,

INTRODUCTION

Polymerase epsilon (POLE) is a major eukaryotic DNA polymerase involved in both DNA replication and repair (1). Its proofreading domain, harboring exonuclease activity, deletes mispaired bases inserted during DNA replication. Mutations that alter the exonuclease domain of POLE and inactivate its editing function lead to the extreme accumulation of missense and nonsense mutations with a very high tumor mutational burden (TMB) with as many as 100 mutations per megabase pair (TMB > 100 mt/Mb; refs. 1–3) with a specific POLE-related mutational single-base substitution (COSMIC SBS10a and 10b) signature >50% (4, 5). A high TMB has been associated with improved outcomes with immune-checkpoint blockade (6, 7), especially in tumors associated with known carcinogens (e.g., tobacco, UV light exposure) and in tumors with DNA repair defects such as mismatch repair deficiency (MMRd; ref. 8).

Defective proofreading *POLE* (*POLE*-pd) mutations are rare and predominantly described in mismatch repair–proficient (MMRp) colorectal and endometrial cancers as sporadic and germline events (2, 9). In general, POLE-pd tumors have a good prognosis (2, 10), and as a result, lower prevalence of *POLE*-pd mutations is expected in the advanced setting. Proofreading defects have been documented for multiple hotspots in the exonuclease domain (D275, P286, S297, N363K, F367, V411, L424, P436, M444, A456, Y458, S459, S461, and A463; refs. 2, 11). However, the functional impact of non-hotspot missense mutations across the *POLE* gene [i.e., variants of unknown significance (VUS)] in terms of the hypermutant phenotype and response to immunotherapy is incompletely characterized (12, 13).

To define the characteristics of *POLE* variants across solid tumors and their impact on the TMB and immunogenomic phenotype, we studied genomic databases across solid tumors and initiated a clinical trial following a two-stage Bayesian enrichment design testing the role of PD-1 blockade in *POLE*-mutated tumors. Cases were identified using a nationwide (France) prospective screening protocol for *POLE* variants, and proofreading deficiency was assessed by an *ad hoc* centralized molecular tumor board. Nivolumab (240 mg i.v. once every 2 weeks) was administered until disease progression [progressive disease (PD)], until toxicity, or up to 2 years. The primary endpoint was the objective response rate (ORR) assessed by RECIST v1.1 at 12 weeks. A secondary endpoint was to assess if POLE-pd led to improved outcomes.

RESULTS

Immunogenomic Analyses of *POLE* Mutations across Solid Tumors

According to the Memorial Sloan Kettering Cancer Center (MSKCC) Integrated Mutation Profiling of Actionable Cancer Targets (IMPACT) molecular screening program, *POLE* alterations are observed in 3.4% of all solid tumors (Fig. 1A), but *POLE*-pd variants account for only 0.4% of mutations and 0.1% in the advanced setting. Most *POLE* variants are benign, VUS, or located outside the exonuclease domain. These *POLE* VUS or nonpathogenic mutations are most often observed in high-TMB tumors such as melanoma, lung, or microsatellite instability–high (MSI-H) tumors, and likely represent passenger mutations rather than oncogenic drivers (Supplementary Figs. S1A–S1D and S2A–S2D; Supplementary Tables S1–S3). Crossing The Cancer Genome Atlas (TCGA) and IMPACT databases, we confirmed that *POLE*-pd mutations are mostly observed in endometrial cancer and colorectal cancer but also found in other gastrointestinal tract, glial, urothelial, prostate, and gynecologic cancers (Fig. 1B; Supplementary Tables S1 and S2). Patients with POLE-pd tumors are younger than other patients (Supplementary Table S3), and in gastrointestinal cancers POLE-pd is mainly observed in male patients (Supplementary Table S2C). Occasionally, we observed that MSI-H tumors could present concomitant POLE-pd, with alternative hotspots and amino acid substitutions compared with microsatellite-stable (MSS) tumors (Fig. 1C; Supplementary Fig. S2C and S2D). In MSS tumors, the most common variants are P286R and V411L. POLE-pd is associated with an ultramutated phenotype in both MMRd/MSI-H and MMRp/MSS tumors, with a mutation burden significantly higher than other tumors harboring other *POLE* alterations (Fig. 1D; Supplementary Tables S1 and S3). Only one *POLE*-pd variant, L424V, usually germline and associated with polyposis (14), was observed in a low TMB tumor (Fig. 1D). Analysis of samples with multiple *POLE* alterations showed that all *POLE*-pd variants were monoallelic without evidence of loss-of-heterozygosity ($N = 96$). Allelic frequency (AF) of *POLE*-pd variants showed a positive correlation with TMB, whereas no correlation was observed for nonpathogenic variants (Supplementary Fig. S1C).

To study the specifics of POLE-pd tumors, Pan-Cancer TCGA RNA-sequencing (RNA-seq) analyses of immune infiltrates and related pathways were performed comparing tumors harboring *POLE*-pd variants or other *POLE* alterations, accounting for TMB and microsatellite status (Fig. 1E; Supplementary Table S4). While POLE-pd tumors did not display higher cytotoxic T-cell infiltrate than other *POLE*-mutated tumors, they had the highest Th1 infiltrate and higher *PD-1* (*PDCD1*) expression compared with other MSS tumors. *PD-L1* (*CD274*) expression was decreased compared with MSS TMB-high tumors, a subgroup composed mainly of melanoma and lung cancers.

To further assess the immune landscape of MSS POLE-pd tumors, we investigated the RNA-seq data of the colorectal TCGA cohort, comparing with MSS non-*POLE* tumors

Boulogne-Billancourt, France. [31]R&D Department, Unicancer, Paris, France. [32]Biostatistics, Hôpital St Louis, Paris, France. [33]U1015 and CIC1428, Institut National de la Santé et de la Recherche Médicale (INSERM), Villejuif, France. [34]Faculté de Médecine, Université Paris Saclay, Le Kremlin-Bicetre, France.

Note: Supplementary data for this article are available at Cancer Discovery Online (http://cancerdiscovery.aacrjournals.org/).

P. Saintigny and S. Chevret contributed equally to this article.

Corresponding Authors: Benoit Rousseau, Department of Medicine, Solid Tumor Division, Mortimer B. Zuckerman Research Center, Memorial Sloan Kettering Cancer Center, 417 E. 68th Street, New York, NY 10065. Phone: 646-888-3998; E-mail: rousseab@mskcc.org; and Aurelien Marabelle, Département d'Innovations Thérapeutiques et Essais Précoces, 114 Rue Edouard Vaillant, 94805 Villejuif, France. Phone: 33-(0)1-42-11-55-92; E-mail: aurelien.marabelle@gustaveroussy.fr

Cancer Discov 2022;12:1435–48

doi: 10.1158/2159-8290.CD-21-0521

Pan-Cancer IMPACT	# Samples	*POLE* alteration total	Pathogenic missense	Nonpathogenic or unknown
All stage	43,680	1,469 (3.4%)	167 (0.4%)	1,302 (3.0%)
Metastasis	15,672	533 (3.4%)	13 (0.1%)	520 (3.3%)

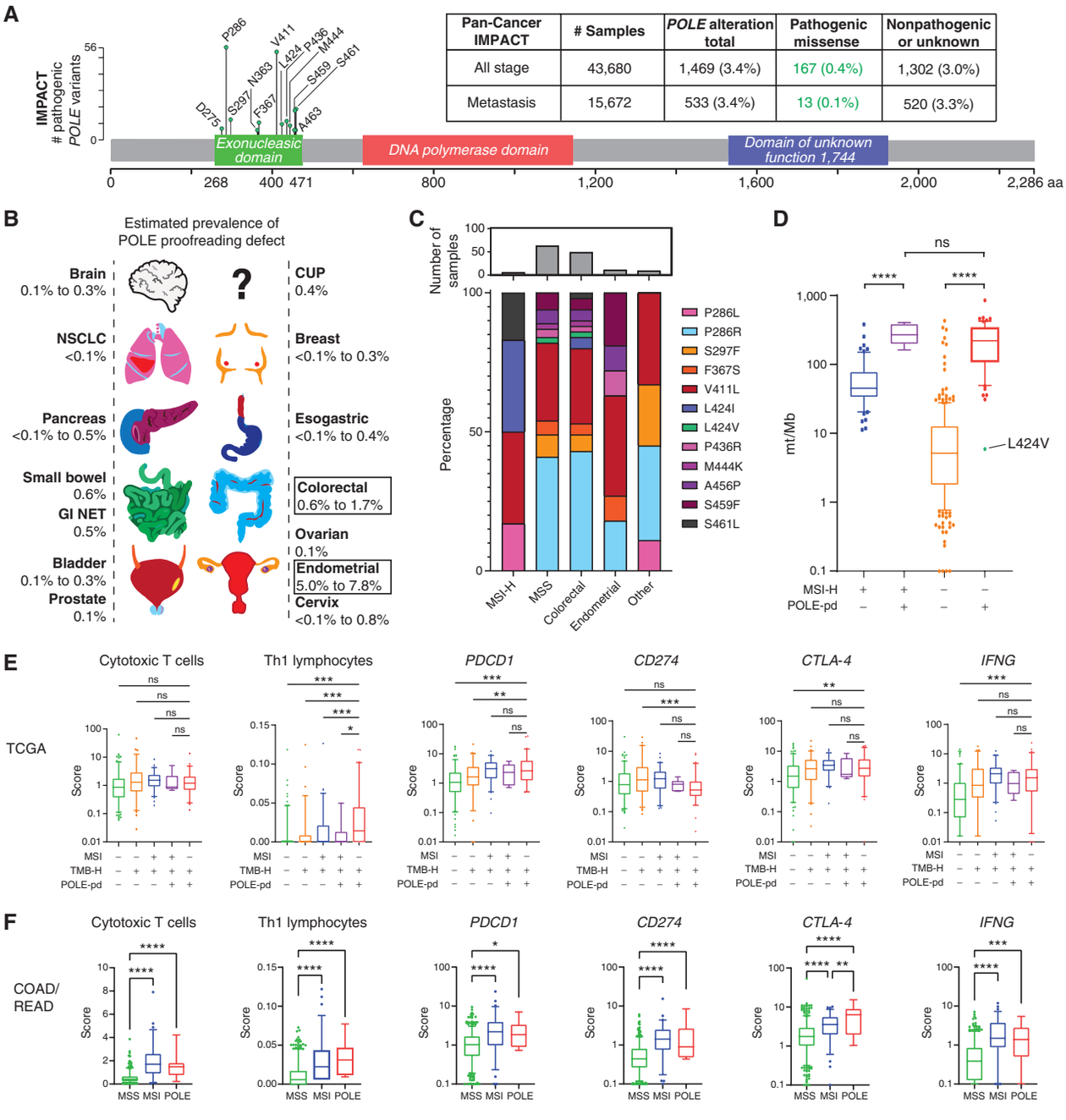

Figure 1. Epidemiology and immunogenomic landscape of solid tumors harboring POLE proofreading defects. **A,** Prevalence of *POLE* pathogenic missense variants leading to proofreading deficiency and other *POLE* molecular alterations in the MSK-IMPACT database from primary tumor samples (all stages) and from metastatic samples. *POLE* hotspot mutations cluster in the exonucleasic domain ranging from amino acid (aa) 268 to 471. **B,** Estimated prevalence of *POLE* proofreading deficiency in solid tumors based on results from the Pan-Cancer TCGA and MSK-IMPACT databases. CUP, carcinoma of unknown primary; NSCLC, non–small cell lung cancer; GI NET, gastrointestinal neuroendocrine tumor. **C,** Prevalence of individual missense proofreading-deficient variants according to microsatellite status and tumor primary in the Pan-Cancer TCGA database. Top, total number of samples in each group. **D,** Mutational burden according to microsatellite status and type of *POLE* alteration in the Pan-Cancer TCGA database. *POLE*-pd, *POLE* proofreading-deficient variants. **E,** Selected immune cell quantification and related genes according to TMB, microsatellite status, and POLE alteration in the Pan-Cancer TCGA database. Statistical comparisons are adjusted for multiple comparisons using POLE-pd MSS tumors as a reference. Additional and numerical results are available in Supplementary Table S4. From left to right, cytotoxic T cells (MCPcounter); Th1 lymphocytes (XCELL); *PDCD1*, programmed cell death 1 gene; *CD274*, programmed cell death ligand 1 gene; *IFNG*, interferon gamma gene; *P* values: ns, nonsignificant; >0.05; *, ≥0.05 and >0.01; **, ≤0.01 and >0.001; ***, ≤0.001 and >0.0001. **F,** Selected immune cell quantification and related genes of colorectal cancer tumors from the COAD/READ database of the TCGA according to microsatellite and POLE-pd status. Statistical comparisons are adjusted for multiple comparisons using POLE-pd MSS tumors as a reference. Additional and numerical results are available in Supplementary Table S4. From left to right, cytotoxic T cells (MCPcounter); Th1 lymphocytes (XCELL); *PDCD1*, programmed cell death 1 gene; *CD274*, programmed cell death ligand 1 gene; *IFNG*, interferon gamma gene; *P* values: ns, nonsignificant, >0.05; *, ≥0.05; >0.01; **, ≤0.01 and >0.001; ***, ≤0.001 and >0.0001; ****, ≤0.0001.

and MSI-H tumors (Fig. 1F; Supplementary Table S5). Our analyses showed that POLE-pd tumors have a high cytotoxic Th1 T-cell infiltrate in line with higher *PD-1* (*PDCD1*) expression. The POLE-pd tumor microenvironment also demonstrates strong upregulation of *IFNG, PD-L1* (*CD274*), and *CTLA-4* compared with MSS tumors, which resembles that seen in MSI-H tumors. Altogether, these data suggest that MSS POLE-pd tumors are good candidates for immune-checkpoint blockade.

Nivolumab Efficacy in Patients with Advanced Solid Tumors Harboring *POLE* Mutations

From January 2018 to December 2020, 61 patients harboring *POLE* mutations had been screened nationwide and assessed by the *ad hoc* molecular board (Fig. 2A). Twenty-one patients were enrolled in cohort 6 of Acsé Nivolumab, dedicated to patients harboring *POLE* mutations and excluding patients with MSI-H tumors or any MSS solid tumor types for which immunotherapy was currently available, such as melanoma and lung cancers. As TMB is not an approved biomarker for immunotherapy in Europe and is not routinely assessed, the molecular board assessed pathogenicity of *POLE* variants blinded to any TMB results. Twenty patients received at least one dose of nivolumab and were further considered for the efficacy analysis.

Clinical characteristics of included patients are summarized in Fig. 2B, and *POLE* variants are detailed in Fig. 2C. The median follow-up was 13.1 months (range = 0.5–26.1 months).

An *ad hoc* committee confirmed the pathogenicity of the *POLE* variants in the tumors of 12 (57%) patients, including three patients with P286R, three with V411L, two with N363K, two with S459F, one with S297Y, and one with A463V mutations, then classified as *POLE*-pd (Fig. 2C; Supplementary Table S6). Of note, one N363K variant was germline. Four patients had VUS, and five had *POLE* proofreading–proficient (POLE-pp) variants (Fig. 2B and C).

Figure 2D and E report, respectively, best response and RECIST target changes at each radiologic assessment. The trial achieved its primary objective with a 38% (7/19) ORR at 12 weeks, which was comprised of seven partial responses (Fig. 2F). Two patients had further complete response as best responses. The 12-week disease control rate (DCR) was 58% (11/19), with four patients maintaining stable disease. One additional patient had stable disease after initial radiologic progression. The safety profile of nivolumab was in accordance with safety data reported in other tumor types (Supplementary Table S7), and one patient stopped nivolumab for serious adverse events.

Responses were observed exclusively in patients with MMRp/MSS colorectal cancer ($N = 5$) and endometrial cancer ($N = 2$). In the overall cohort, median progression-free survival (mPFS) and median overall survival (mOS) were 5.4 months (Fig. 2G) and not reached, respectively (Fig. 2H).

Figure 2I displays a nearly complete response observed in a 42-year-old patient with an unresectable transverse colon tumor with a POLE-pd P286R variant. This response allowed resection of the residual lesion and revealed a 4.2-cm-long, pan-parietal mass with a mucoid aspect (Supplementary Fig. S3A and S3B). The pretreatment tumor (Supplementary Fig. S4A–S4D) was rich in tumor-infiltrating lymphocytes (TIL) and $CD8^+$ cells and had low PD-L1 expression. The posttreatment lesion displayed mucoid pools without tumor cells, dissociated by trabeculae of paucicellular fibrosis, and was enriched in $CD8^+$ cells (Supplementary Fig. S4E–S4H). There were also foci of infarctoid necrosis bordered by macrophagic cells (Supplementary Fig. S4I–S4L).

Activity of Nivolumab According to POLE Proofreading Defect

We investigated the impact of the prospectively determined *POLE* proofreading defect on nivolumab benefit. Whole-exome sequencing (WES) was successfully performed on 14 tumors, providing TMB and SBS signatures for pathogenicity confirmation. Two more patients had TMB results thanks to panel sequencing performed before inclusion in the trial.

Figures 2D and 3 display the overall results stratified by pathogenicity, TMB, and SBS POLE signatures. Sequencing confirmed that all *POLE*-pd variants were monoallelic, whereas other nonpathogenic mutations could be observed simultaneously.

TMB assessment confirmed that the pathogenicity assessed by the molecular board was concordant in 100% (10/10) of

Figure 2. Primary endpoint results for the POLE cohort of the Acsé Nivolumab trial. **A,** Flow chart of the Acsé Nivolumab POLE phase II trial showing how patients were selected from a nationwide screening strategy, through the eligibility and pathogenicity assessment of each POLE variants by an *ad hoc* molecular board (four molecular biologists and one medical oncologist), and then to the two-stage phase II trial with Bayesian enrichment design. **B,** Summary of clinicodemographic characteristics of enrolled patients in total and according to their proofreading category. PS (ECOG), Performance Status (Eastern Cooperative Oncology Group). **C,** *POLE* variants and pathogenicity according to primary tumor. POLE-pd: +, yes; –, no; ?, VUS. Of note, one variant, N363K, was germline. *, Including one patient with poorly differentiated neuroendocrine rectal cancer. #, One patient with a colorectal cancer and S459F POLE-pd variant was included in the trial but did not receive nivolumab because of rapid clinical deterioration and is further excluded from efficacy analyses. **D,** Best response of target lesions according to an independent review committee (IRC) RECIST v1.1 assessment presented by primary tumor and according to molecular features, POLE proofreading category, TMB, and COSMIC POLE SBS signature. POLE-pd: +, yes; –, no; ?, VUS. TMB-high: +, TMB ≥10 mt/Mb; –, TMB <10 mt/Mb; NA, not available. POLE SBS, proportion of POLE-related SBS assessed by WES: +, POLE SBS signature >60%; ±, POLE SBS signature >1% and ≤60%; –, POLE SBS signature of 0%; #, low cellularity of the sample; NA, not available. CR, complete response; PR, partial response; SD, stable disease. Three patients experienced early clinical progression, and one withdrew consent after cycle 1 of nivolumab and did not perform a CT scan, so the total number of patients displayed is 16. **E,** Volume change of target lesions at each radiologic assessment according to IRC RECIST v1.1 presented by primary tumor. Three patients experienced early clinical progression, and one withdrew consent after cycle 1 of nivolumab and did not perform a CT scan, so the total number of patients displayed is 16. **F,** Radiologic responses according to IRC RECIST v1.1 assessment at 12 weeks (primary endpoint) and best response in the overall cohort. DCR at 12 weeks, disease control rate at 12 weeks according to IRC RECIST v1.1; ORR at 12 weeks, overall response rate according to IRC RECIST v1.1; PD, progressive disease. One patient withdrew consent after one cycle of nivolumab and was not assessable for response. *, Three patients who experienced early clinical progression have been classified as progressors. **G,** PFS curve from the initiation of nivolumab in the overall POLE cohort ($N = 20$). **H,** OS curve from initiation of nivolumab in the overall POLE cohort ($N = 20$). **I,** Abdominal CT scan showing pretreatment and 12 weeks after nivolumab the nearly complete response of a patient with unresectable locally advanced transverse colon cancer with a POLE-pd P286R variant. The red circles highlight a target lesion and its evolution between baseline and after nivolumab.

A

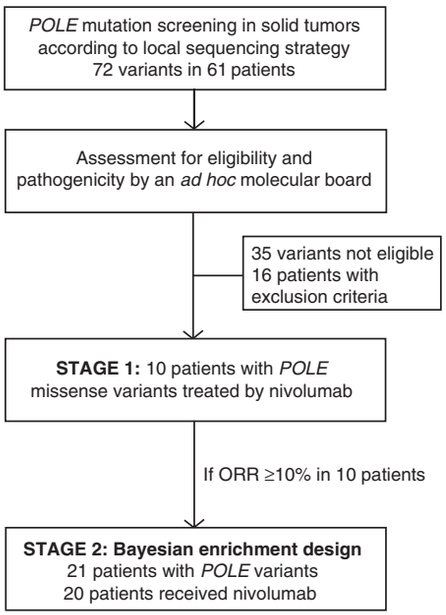

B

		POLE proofreading category		
	All ***N*** **= 21**	**POLE-pp** ***N*** = 5	**VUS** ***N*** = 4	**POLE-pd** ***N*** = 12
Age, years	57 ± 16	64 ± 10	56 ± 16	54 ± 17
Sex (male)	12 (57%)	5 (100%)	2 (50%)	5 (42%)
PS (ECOG) = 1	16 (75%)	4 (80%)	2 (50%)	10 (83%)
Primary tumor				
*Colorectal**	9 (43%)	2 (40%)	2 (50%)	5 (42%)
Endometrial	6 (29%)	0 (0%)	0 (0%)	6 (50%)
Gastric	2 (9%)	2 (40%)	0 (0%)	0 (0%)
Glioblastoma	1 (5%)	0 (0%)	0 (0%)	1 (8%)
Biliary tract	1 (5%)	0 (0%)	1 (25%)	0 (0%)
Pancreas	2 (9%)	1 (20%)	1 (25%)	0 (0%)
Previous treatments (*N*)	2.4 ± 2	5 ± 2	1.8 ± 1	1.5 ± 1

C

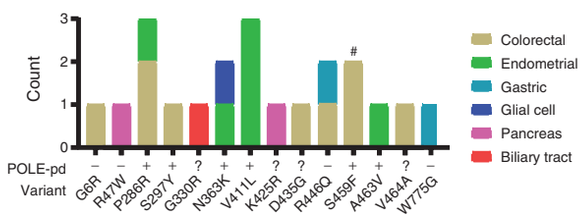

D

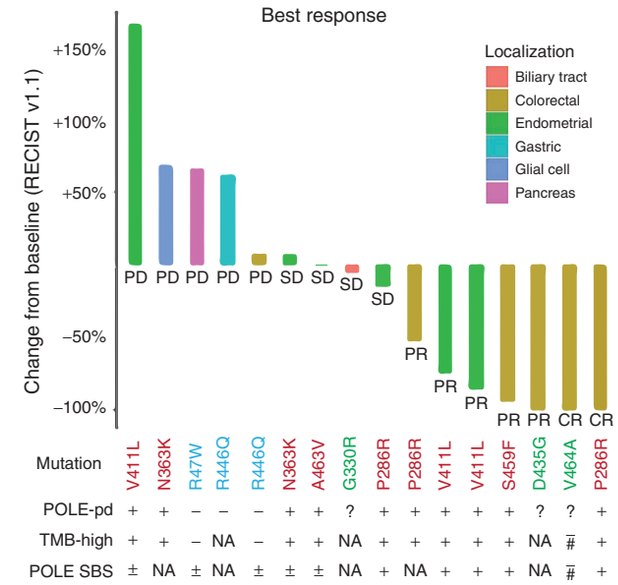

E

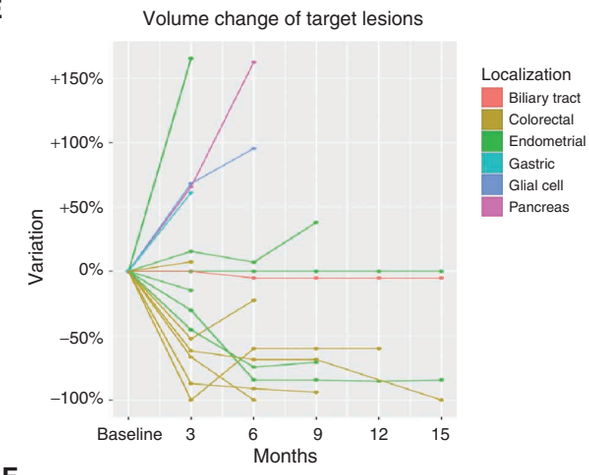

F

RECIST v1.1	**Response at 12 wk % (*n*/*N* = 19)**	**Best response % (*n*/*N* = 19)**
ORR (PR + CR)	37% (7)	37% (7)
DCR (SD + PR + CR)	58% (11)	58% (11)
PD*	42% (8)	42% (8)

G

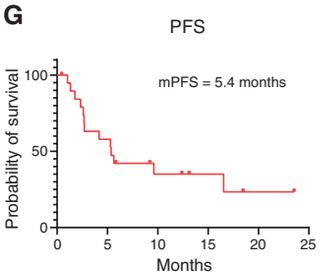

H

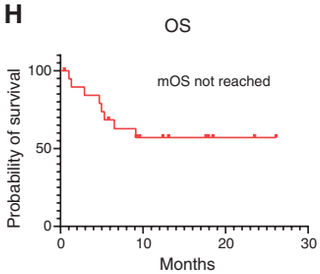

I

POLE-pd instances (Figs. 2D and 3A), as all displayed high TMB (median of 114 mt/Mb, min: 25, max: 385). In the same line of evidence, 100% (3/3) of the POLE-pp tumors had low TMB (median of 5 mt/Mb, min: 4, max: 9). Only two tumors with VUS were successfully sequenced, with both displaying low TMB (median of 3 mt/Mb, min: 2, max: 4); of note the patient with the V464A variant had low cellularity possibly impairing TMB assessment.

Study of the POLE SBS signature showed that all POLE-pd tumors had a typical POLE mutational profile (100%, 8/8; Figs. 2D and 3B). Among these POLE-pd tumors, we observed a wide variation in the proportion of POLE SBS signature (median 67%, min: 18%, max: 80%). Interestingly, two tumors with *POLE*-pp variants showed an attenuated POLE SBS signature below 15% (R47W and R446Q). The variants G6R, K425R, and V464A had a POLE SBS signature of 0% but surprisingly displayed MMRd SBS signatures >30%, whereas TMB was low, without any argument for MMRd (IHC and/or MSI score).

Then, using RNA-seq, we assessed the immune infiltrates according to proofreading deficiency. We observed that patients with *POLE*-pd/VUS variants had higher $CD8^+$ T-cell infiltrates (Supplementary Fig. S5A and S5B) compared with *POLE*-pp variants. Of note, two patients with VUS (G330R and V464A) and long-lasting control had tumors with high $CD8^+$ T-cell infiltrate.

Among assessable patients with *POLE*-pd mutations, five patients showed responses, for an ORR of 46% (5/11), and an additional 27% (3/11) of patients achieved stable disease, which yielded a DCR of 73%. Best responses were observed early with long-lasting control (Figs. 2E and 3A). Progressions were observed as best response in patients with endometrial cancer and glioblastoma despite having *POLE*-pd variants. Concerning the four patients with VUS, two had responses, one had stable disease, and one progressed. In contrast, at 12 weeks, all five patients with *POLE*-pp variants progressed. According to the Bayesian enrichment design, because no evidence of activity was observed in patients harboring *POLE*-pp mutations after the first 15 included patients, we subsequently enrolled only patients with *POLE*-pd variants or VUS.

Higher TMB was associated with higher likelihood of responses (Fig. 3B). The intensity of the SBS POLE signature was able to discriminate responders, stabilization, and progression (mean of 80%, 60%, and 15%, respectively). Correction of TMB by the amount of SBS POLE signature revealed that responders had the strongest POLE-pd phenotypes with extremely high TMB composed mostly of POLE-related mutations. The study of the AF of *POLE*-pd variants did not show a correlation with response or SBS signature (Supplementary Fig. S6A–S6E), whereas a trend for lower TMB was observed for lower AFs, and an SBS POLE signature <50% was observed only for low allelic variants (Supplementary Fig. S6C). All POLE-pd variants were monoallelic.

Figure 3C and E display PFS and OS results according to TMB and molecular board–assessed pathogenicity. Both TMB and pathogenicity were informative to predict the benefit, and the VUS category seems to present an intermediate benefit. When comparing nonpathogenic and pathogenic/VUS groups, the respective mPFS and mOS were 2.3 versus 9.6 months [HR (PFS) = 0.2; 95% confidence interval (CI) = 0.1–0.7] and 4.7 months versus not reached [HR (OS) = 0.1; 95% CI = 0.02–0.7; Fig. 3D and E). Figure 3F details best responses per variants, pathogenicity class, and related median TMB.

As the main *POLE*-pd mutations were observed in colorectal cancer, we inquired as to the outcomes of POLE-pd patients compared with MMRd/MSI-H patients in an independent cohort of advanced colorectal cancer exposed to single-agent PD-1 inhibitor (N = 35; Supplementary Fig. S7A–S7C). The observed PFS and OS of POLE-pd MMRp patients when exposed to anti–PD-1 was similar to those of MMRd/MSI-H colorectal cancer patients, confirming the benefit observed in this rare population.

In Silico POLE Mutation Pathogenicity Analyses Reveal Two Tridimensional Hotspot Sites Correlating with Benefit from Nivolumab

To assess the functional impact of *POLE* variants on proofreading activity, *in silico* tridimensional analyses combined with DNA affinity models were performed (Fig. 4A; Supplementary Figs. S8 and S9; Supplementary Video S1 and Supplementary Table S8).

The mutations in the exonuclease domain can be spatially and functionally grouped into three categories: (i) residues on the DNA binding side of the exonuclease domain (Fig. 4A, part d); (ii) residues affecting the catalytic core of the exonuclease domain (Fig. 4A, part e); and (iii) surface residues

Figure 3. POLE proofreading deficiency drives benefit from nivolumab. **A,** Swimmer plot of overall survival, time to best response, and time to progression according to primary, *POLE* variant proofreading category, and TMB. *, Patient withdrew consent after one cycle of nivolumab. #, Low tumor purity. +, TMB ≥10 mt/Mb; –, TMB <10 mt/Mb; NA, nonavailable. CR, complete response; PD, clinical or radiologic progressive disease; PR, partial response; SAE, serious adverse event; SD, stable disease. **B,** An independent review committee (IRC) assessment of RECIST v1.1 best response with molecular features. From left to right, TMB, POLE SBS, and POLE signature TMB (TMB value imputable to POLE SBS signature calculated as the product of % of POLE SBS signature and TMB of a specific tumor). *P* values have been calculated using Fisher test. The patient with the V464A VUS variant has not been considered for these analyses because of low tumor purity. *P* values: ns, nonsignificant, >0.05; *, ≥0.05 and >0.01; **, ≤0.01 and >0.001. **C,** PFS and OS curves from start of nivolumab comparing outcomes of patients according to their tumor TMB. *P* value has been computed by the log-rank test. TMB-low, <10 mt/Mb; TMB-high, ≥10 mt/Mb; unknown, not available. **D,** Main oncologic outcomes according to *POLE* variant proofreading category assessed by the molecular tumor board. The three patients without assessment at 12 weeks have been classified as progressors. DCR at 12 weeks, DCR at 12 weeks according to IRC RECIST v1.1; HR (95% CI), HR (95% CI) corresponding to the Cox model comparison of nonpathogenic versus pathogenic/VUS group; ORR at 12 weeks, ORR according to IRC RECIST v1.1. All patients who received at least one dose of nivolumab are considered for survival outcome assessment (N = 20). *, One patient withdrew consent at 2 weeks after one cycle of nivolumab and is not accounted for response but is accounted for survival analyses. **E,** PFS and OS curves from the start of nivolumab comparing outcomes of patients according to their tumor POLE proofreading category. *P* value has been computed by the log-rank test. **F,** Individual responses for each POLE variant classified as POLE-pd, VUS, or POLE-pp and corresponding median TMB for each category. CR, complete response; mTMB: median TMB; NA, not assessed; PR, partial response; SD, stable disease. $, Patient with the V464A variant had low TMB with low tumor purity.

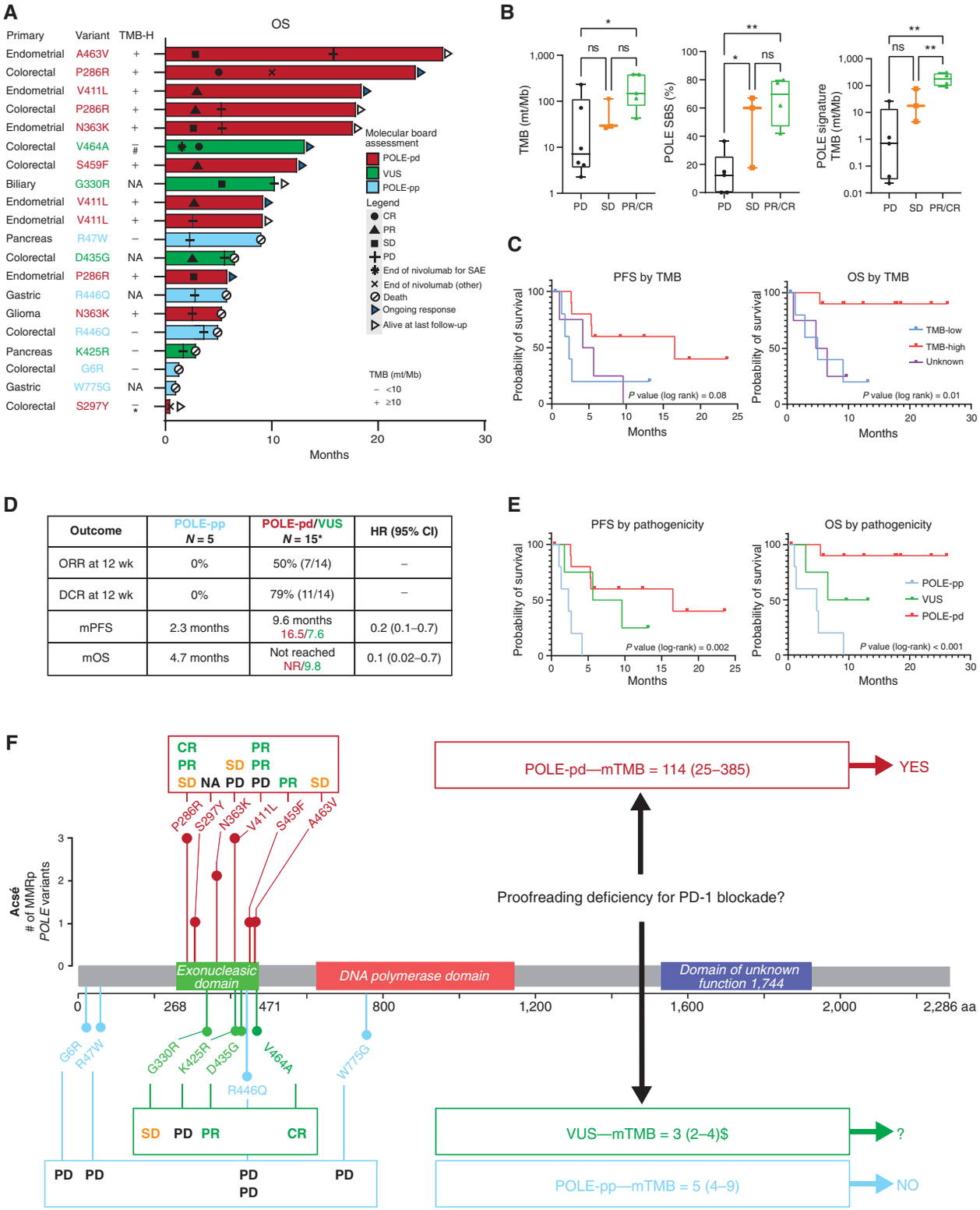

Outcome	POLE-pp *N* = 5	POLE-pd/VUS *N* = 15*	HR (95% CI)
ORR at 12 wk	0%	50% (7/14)	–
DCR at 12 wk	0%	79% (11/14)	–
mPFS	2.3 months	9.6 months 16.5/7.6	0.2 (0.1–0.7)
mOS	4.7 months	Not reached NR/9.8	0.1 (0.02–0.7)

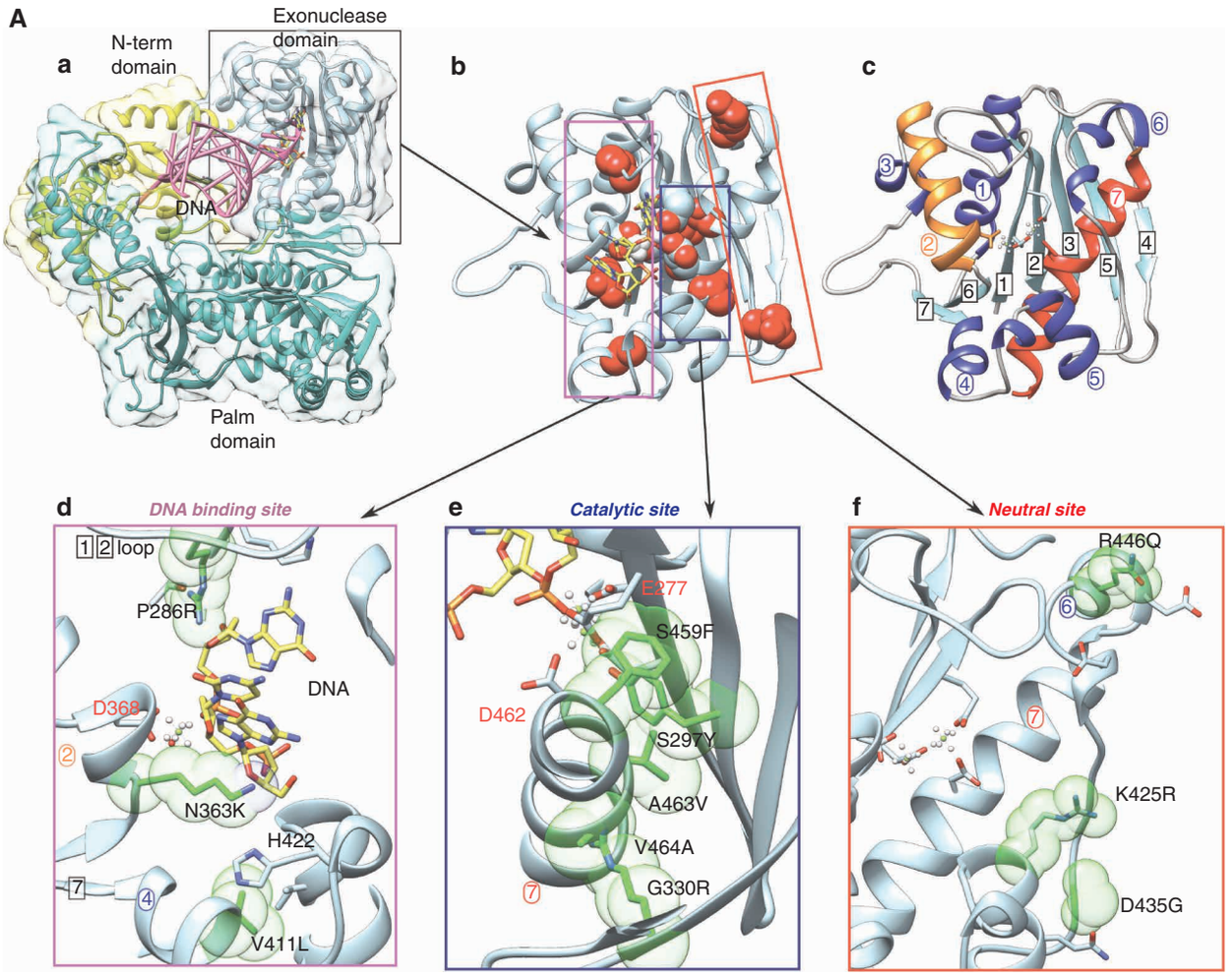

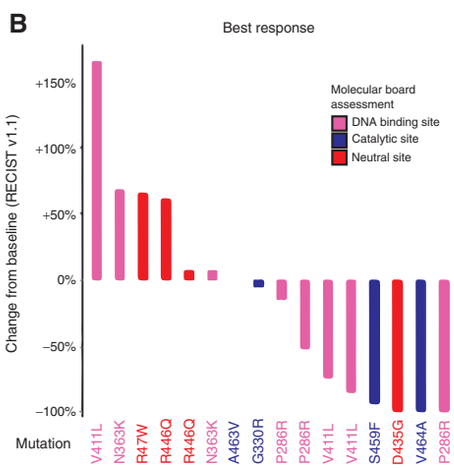

C

POLE domain	ORR	DCR
DNA binding site	50% (4/8)	75% (6/8)
Catalytic site	50% (2/4)	100% (4/4)
Neutral site	14% (1/7)	14% (1/7)

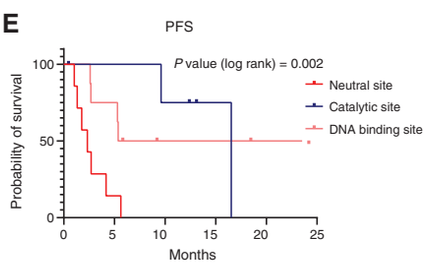

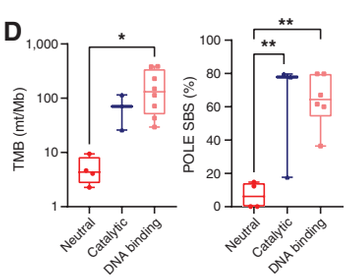

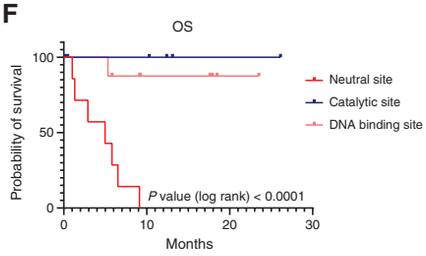

not predicted to hinder exonuclease function (Fig. 4A, part f). Classifying the variants according to their predicted tridimensional site (DNA binding site, catalytic site, or predicted to have a neutral impact as away from the DNA binding or catalytic site; Supplementary Table S7), we assessed the related TMB, POLE SBS signature, and associated benefit derived from nivolumab (Fig. 4B–D). Patients with variants within the catalytic site or the DNA binding site seemed to have a similar benefit (Fig. 4B and C), including two patients with VUS G330R and V464A and long-term benefits who were both recategorized as belonging to the catalytic site thanks to the *in silico* model. In contrast, in the neutral site group, only one response was observed (ORR = 17%), in one patient with a D435G VUS and a short benefit (Fig. 3A).

TMB was high for all variants within the DNA binding and catalytic sites, whereas TMB was low for all the neutral variants (Fig. 4D; Supplementary Fig. S1D). The POLE SBS signature had similar amplitudes for the DNA binding and catalytic site (Fig. 4D). Excellent PFS and OS were observed for patients with tumors harboring DNA binding and catalytic sites variants (Fig. 4E and F), with long-lasting plateaus. To the contrary, patients with tumors having neutral variants showed no sustained benefit.

DISCUSSION

Here we report the first prospective assessment of anti–PD-1 immunotherapy for patients with advanced tumors harboring predefined *POLE* mutations. While the primary endpoint was achieved in the overall population, responses were limited to patients with variants affecting proofreading, clustering in the DNA binding or catalytic sites. Patients were included with blinded TMB values, and similar to MMRd/MSI-H, POLE-pd status alone was sufficient to predict high TMB and benefit from anti–PD-1 therapy (15, 16). Strikingly, tumor types that exhibit high rates of MMRd/MSI-H, including colorectal cancer and endometrial cancer, also exhibit the highest relative prevalence of *POLE*-pd mutations, suggesting that intrinsic DNA repair impairment is a strong biomarker of sensitivity to checkpoint blockade in specific cancer types.

POLE-pd prevalence across solid tumors is extremely low, raising concerns on how to identify them in clinical practice. Large sequencing panels and TMB assessments are not available in clinical routine uniformly worldwide. Our study shows that some tumor types should be considered for POLE testing and provides characterization of variants impairing proofreading. Like MMRd/MSI-H tumors, metastatic MSS samples show low prevalence of POLE-pd because of an excellent prognosis at the early stage. In addition, this trial was supported by the French National Cancer Institute (INCa), which organized and provided guidelines for screening to all national sequencing platforms. Our study highlights how centralized coordinated efforts could help to identify patients with rare molecular alterations in the era of precision oncology.

Our Pan-Cancer analyses, combined with a clinical trial designed to include only patients with tumor types not eligible otherwise for immunotherapy, helped us to better understand how *POLE* mutations and TMB are intertwined. First, we confirmed that *POLE*-pd variants causing DNA repair impairment and high POLE-related TMB were exclusively monoallelic missense variants clustering in DNA binding and catalytic domains. Second, we showed that neutral missense mutations could be secondary to other hypermutability processes, as observed in UV light– or tobacco-driven tumors, displaying usually high sensitivity to immune-checkpoint blockade in line with their TMB and PD-L1 expression. Finally, we showed prospectively for the first time that tumors with *POLE* neutral missense variants in classically low-TMB

Figure 4. *In silico* analyses reveal two tridimensional hotspot sites correlating with benefit from PD-1 blockade. **A,** *In silico* model of mutations located in the exonuclease domain. (a) Overall structure of POLE showing all the domains with the exception of the thumbs domain for clarity as well as a zoomed-in view of the exonuclease domain in the same orientation. The DNA is modeled in the editing conformation. (b) exonuclease domain with mutations represented in red spheres. (c) Topology of the exonuclease domain, with the β strands numbered in square boxes and α helices in rounded boxes. The α helices contributing to the catalytic site (2 and 7) are colored orange and red. Mutations, represented in green, (d) found in the DNA binding groove (e) found in the hydrophobic core near the catalytic site (f) in surface residue mutations away from the functional sites, expected to have a neutral impact. The exonuclease domain (Fig. 4A, parts a–c) has a β1, β2, β3, β4, β5, α1, β6, α2, α3, β7, α4, α5, α6, and α7 topology. The β strands form a central β-sheet, and the C-terminal α7 helix (red in Fig. 4A, part c) packs on the interior side of the β-sheet to form the main hydrophobic core of the protein. The metal binding residues of the catalytic site are located on β1, β2, α2 (orange in Fig. 4A, part c), and α7. The predicted DNA binding site is located in the groove lining the active site, with α2 and α7 on the left and right and the β1–β2 loop and α4–α5 bundle on the top and bottom in the orientation of Fig. 4A, part c. The P286, N363, and V411 residues, located in the β1–β2 loop, in α2 and in α4, respectively, line the DNA binding site in the exonuclease domain (Fig. 4A, part d, and Supplementary Fig. S8). Mutations of these residues are predicted to either interfere directly with DNA binding (N363K) or indirectly by destabilizing structural elements in contact with the DNA (P286R and V411L). The N363 residue is also near the metal binding site (in the same helix as D368), and the mutation to a basic lysine residue could also destabilize the metal binding of the acidic active site residues. The S297, G330, S459, A463, and V464 residues cluster in the hydrophobic core formed between the α7 helix and the β-sheet (Fig. 4A, part e, and Supplementary Fig. S8). In addition to the general destabilization of the protein by disruption of the hydrophobic core, the close proximity of these mutations with the metal binding residues of the β1 (S459, E277) and α7 (D462) residues will have a direct effect on the catalytic activity of the enzyme. This region appears as a mutation hotspot with pathogenic consequences. K425, D435, and R446 are surface residues far away from the active site (Fig. 4A, part f, and Supplementary Fig. S9). The mutations of these residues could disrupt salt bridges with neighboring residues but are not predicted to directly interfere with exonuclease function. R47 and W775 are not found in the exonuclease domain but belong to the N-terminal and thumb/finger domains, respectively (Supplementary Fig. S9). None of these mutations are predicted to impact the function of the exonuclease domain. **B,** Summary of best response observed in the Acsé trial according to the POLE-variant tridimensional site predicted by *in silico* analyses: DNA binding site, catalytic site, or neutral site. **C,** Radiologic best responses according to an independent review committee RECIST v1.1 assessment for tridimensional categories of POLE variants in DNA binding, catalytic, or neutral site. The three patients who experienced early clinical progression have been classified as progressors all in the neutral site category. One patient withdrew consent after one cycle of nivolumab and was not assessable for response (catalytic site variant). **D,** Correlation of molecular features with tridimensional categories. From left to right, TMB, POLE SBS, and POLE signature TMB (TMB value imputable to POLE SBS signature calculated as the product of % of POLE SBS signature and TMB of a specific tumor). *P* values have been calculated using Fisher test. The patient with the V464A VUS variant has not been considered for these analyses because of low tumor purity. *P* values: *, ≥0.05 and >0.01; **, ≤0.01 and >0.001. **E,** PFS observed in the Acsé trial according to the POLE-variant site predicted by *in silico* analyses: DNA binding site, catalytic site, or away from these sites. *P* value corresponds to a log-rank test. **F,** OS observed in the Acsé trial according to the POLE-variant site predicted by *in silico* analyses: DNA binding site, catalytic site, or away from these sites. *P* value corresponds to a log-rank test.

tumors derived no benefit from PD-1 blockade, providing nuance to previous retrospective reports (12, 17). Altogether, these results highlight the need for careful joint assessment of POLE pathogenicity and TMB if available to avoid unnecessary and potentially harmful treatment by immunotherapy.

Tridimensional assessment of *POLE* variants seems to provide additional predictive value. Indeed, PFS and OS of patients with *POLE* DNA binding or catalytic sites mutated tumors were significantly improved compared with patients with tumors mutated in *POLE* away from these tridimensional sites. Our results also suggest that patients with tumors harboring missense VUS within *POLE* DNA binding and catalytic sites may derive a benefit from immunotherapy, whereas TMB and mutational signature assessments did not confirm their pathogenicity. Responsive patients with VUS in the Acsé trial could correspond to rare POLE variants with an attenuated phenotype. This hypothesis remains to be confirmed in a larger cohort and *in vivo* functional studies.

Translational analyses showed that POLE-pd tumors present with a strong T-cell infiltrate, immune-checkpoint expression, and high IFNγ. In this study, we also confirmed that advanced POLE-pd tumors presented with high $CD8^+$ T-cell infiltrates compared with POLE-pp variants. Interestingly, patients with tumors harboring *POLE* VUS within the DNA binding/catalytic site also had a high $CD8^+$ T-cell infiltrate.

WES allowed us to study the relationship between response to PD-1 blockade and molecular features of *POLE*-mutated tumors. TMB and pathogenicity assessed by the molecular board were perfectly congruent. All patients benefiting from nivolumab had tumors with high TMB, except from one with low cellularity. Inversely, two patients (19%) with high TMB had progression as best response. COSMIC POLE-related SBS signature assessment revealed that responses correlated with higher proportion of POLE-related SBS mutations, measuring the intensity of the proofreading defect phenotype. The most benefiting patients had high TMB with more than 60% of their mutations attributable to POLE proofreading defect. The study of AFs of POLE-pd variants showed that response could be observed if the *POLE* variant was clonal (AF ≥10%) or subclonal (AF <10%). Subclonal cases tended to have lower TMB and lower SBS POLE signature, suggesting that late emergence of a POLE-pd variant could lead to an attenuated phenotype. These data are in accordance with recent reports that specific mutational processes are highly immunogenic (18), confirming that the intensity of the POLE proofreading defect drives immunogenicity not only in MMRd/MSI-H tumors (19) but also in a pure MMRp/MSS context.

Altogether, this study showed that *POLE*-pd mutations predict high activity from anti–PD-1 in MMRp/MSS solid tumors and should be considered as a new tumor-agnostic biomarker for PD1-blockade immunotherapy. *POLE*-pd mutations lead to TIL-rich ultramutated tumors highly benefiting from immunotherapy. To the contrary, MMRp/MSS tumors with *POLE* mutations not affecting proofreading derived no benefit in tumor types that are classically considered poorly responsive to PD-1 blockade. This trial supports the idea to extend the concept of an agnostic predictive biomarker for checkpoint blockade of MSI to a larger set of tumors with intrinsic DNA repair impairment, MMRd/MSI-H, and/or POLE-pd.

METHODS

Acsé Nivolumab

Acsé Nivolumab is a multicenter (n = 46 sites) phase II basket trial sponsored by INCa (www.e-cancer.fr) and the French network of comprehensive cancer centers (Unicancer; www.unicancer.fr) investigating in multiple single-arm cohorts the efficacy of anti–PD-1 immunotherapy in rare tumor types. Version 1.1 from January 30, 2017, of the protocol was approved by the Agence Nationale de Sécurité du Médicament on February 10, 2017 (EUDRACT #2016-002257-37), was approved by the ethical committee "Comité de Protection des personnes (CPP) Ouest II (Angers)" on February 16, 2017 (#CPP 2017/02), and declared on ClinicalTrials.gov on January 6, 2017 (NCT03012581). Written informed consent was obtained from all the patients. The POLE cohort of the Acsé Nivolumab trial allowed the inclusion of patients with solid tumors harboring a missense *POLE* mutation, according to local sequencing methods, prospectively categorized for pathogenicity by an *ad hoc* centralized molecular board as POLE-pd, non–POLE-pp, or VUS. The main inclusion criteria were Eastern Cooperative Oncology Group Performance Status ≤1, advanced MMRp/MSS tumors confirmed by local IHC and/or PCR, tumors refractory to standard therapies, without prior exposure to immune-checkpoint inhibitors and/or without a primary tumor having an active approval for immunotherapy. Nivolumab (240 mg i.v. once every 2 weeks) was administered until disease progression (PD), until toxicity, or up to 2 years.

The primary endpoint was ORR assessed by RECIST v1.1 at 12 weeks by an independent review committee (IRC). Secondary endpoints included tolerance (Common Terminology Criteria for Adverse Events v4.0), best response, PFS, OS, and subgroup analyses according to proofreading defect.

The provision of baseline tumor material was mandatory per protocol at enrollment. Therefore, all patients included in the Acsé nivolumab trial consented to provide blood and either provide archival tumor material (less than 6 months old) or underwent a *de novo* tumor biopsy during the screening period for subsequent ancillary analysis. Pretreatment frozen peripheral blood mononuclear cells (PBMC; germinal material) and formalin-fixed, paraffin-embedded (FFPE) tumor blocks (somatic material) were submitted for DNA and RNA extraction, followed by WES and RNA-seq.

Design

The trial used a two-stage Bayesian enrichment design, which allowed for a smaller more informative trial that is specifically tied to decision-making within a drug development program. This process allowed for incremental changes to each cohort based on current data rather than restricting revisions in a trial design using fixed sample sizes (20, 21).

The first stage led to an interim analysis of the primary endpoint (ORR at 12 weeks), which was planned after 10 patients were enrolled in the cohort and completed the first scheduled disease evaluation. Based on an expected minimal ORR of 10% (85% confidence), the cohort continued only if at least one patient presented a radiologic response out of 10. For the second stage, intracohort analyses were performed after every five additional patients accrued (20). These analyses used all data accumulated up to that point and considered potential predictive markers of efficacy such as POLE pathogenicity assessment. Subset analyses allowed identification of subcohorts of poor outcomes that may be proposed for enrollment discontinuation, whereas those with good outcomes could enrich the design (22).

POLE *Variant Classification*

In the Pan-Cancer analyses, *POLE* pathogenicity was classified according to Campbell and colleagues (2) and enriched by other well-described pathogenic variants from the literature (Supplementary

References). Considered pathogenic missense variants, whatever the amino acid substitution, were D275, P286, S297, N363, F367, V411, L424, P436, M444, A456, Y458, S459, S461, and A463.

Variants observed in the Acsé trial were classified prospectively according to the American College of Medical Genetics and Genomics standards and guidelines for the interpretation of sequence variants (23). A detailed description of the variants included in the trial and their classification is given in Supplementary Table S6.

DNA and RNA Extraction

Genomic DNA was extracted from FFPE tissues using the Maxwell 16 FFPE Plus LEV DNA Purification Kit (Promega) and from blood samples using the QIAamp Mini Kit (Qiagen) following the manufacturers' instructions. DNA concentration was dosed by a Qubit fluorometer (Invitrogen), absorbances were analyzed by a NanoDrop spectrophotometer (Thermo Fisher Scientific), and quality profiles were assessed on Tapestation (Agilent Technologies).

Total RNA from FFPE tissues was extracted using FormaPure RNA (Beckman Coulter). RNA concentration and absorbances were analyzed with a NanoDrop spectrophotometer (Thermo Fisher Scientific), and quality profiles were assessed on Tapestation (Agilent Technologies).

WES and RNA-seq

Whole exome was captured from a FFPE, and paired constitutional DNA and libraries were prepared with Agilent SureSelect XTHS2 All Exon v8 (42 Mb) reagent kits according to the manufacturer's protocols (Agilent Technologies). Libraries were sequenced on a NovaSeq 6000 Illumina sequencer in 100-bp paired-end reads (Illumina).

For RNA-seq, libraries were prepared with the TruSeq Exome Kit following recommendations (Illumina) and sequenced on a NovaSeq 6000 sequencer in 75-bp paired-end reads.

WES Bioinformatics Analysis

All exome sequencing data were mapped to the hg38 human reference genome with bwa aligner v0.7.15-r1140 (https://github.com/lh3/bwa). Alignments were sorted and duplicates were marked using biobambam v2.0.79 (https://gitlab.com/german.tischler/biobambam2).

Somatic point mutations and short indels were called using the Mutect2 module from GATK v4.1.2 (https://github.com/broadinstitute/gatk). The genome aggregation database gnomAD v2.1.1 was used as a resource to calibrate variant calling model in Mutect2. Also, a panel of 80 normal samples sequenced on the same sequencing machine (NovaSeq6000) was used to remove recurring sequencing artifacts. All variants were annotated using the ensembl-vep v98.3 annotation tool, which integrates COSMIC v89 and dbSNP v152 resources in its cache.

TMB was computed from nonsynonymous variants (point mutations or indels) on the exome target with a variant allele frequency of at least 5% and is reported in mt/Mb.

SBS10 mutation signatures (SBS 10a + 10b corresponding to POLE proofreading defect) and MMRd signatures (4) were computed using SigProfilerSingleSample (COSMIC mutational signature V3; https://github.com/AlexandrovLab/SigProfilerSingleSample).

MSI status was determined using MSIsensor-v0.6 (24) using a list of 2,932 manually curated sites (25). Tumor samples were assigned an MSI-high status when more than 20% of tested loci were unstable.

Translational Analyses and Data Source

Clinicogenomic data were extracted from the Pan-Cancer TCGA and the MSK-IMPACT databases on cBioPortal [Institutional Review Board (IRB) Protocol 12-245; refs. 26–28]. Microsatellite status was determined in both cohorts using the MSI sensor score, considering MSI-H with a score ≥10 and MSS with a score <10. For TCGA, the thresholds of 10 mt/Mb and 100 mt/Mb were used to define hypermutated tumors and ultramutated tumors, respectively, as previously described (2). Bulk RNA-seq data from the TCGA series were downloaded for the COAD/READ cohorts and for available samples harboring *POLE* alterations across all tumor types.

RNA-seq Bioinformatics Analysis and Immune Deconvolution of Bulk RNA-seq Data

Alignments were performed using STAR (version 2.7.10a) on the hg38 human reference genome. FastQC (version 0.11.9) and MultiQC (version 1.12) were used for quality control.

Analyses were carried out using R system software, version 4.0.3. TCGA expression matrices corresponded to unnormalized counts aggregated by HUGO gene symbol. We normalized these data using an original R script implementing the TPM algorithm (29). We then $\log_2$-transformed the TPM normalized data after adding 1e−5 to these data; in the resulting $\log_2$ TPM-normalized matrices, we set to zero the negative values. As TPM uses the length of the genes, we used the biomaRt R package to get this information from the Ensembl Homo sapiens gene database (version 105). We then performed immune cell–type deconvolution of the $\log_2$ TPM data, according to three algorithms: MCPcounter (30), implemented in the MCPcounter R package (https://github.com/ebecht/MCPcounter); XCELL (31); and EPIC [ref. 32; both xCELL and EPIC implemented in the immunedeconv R package (https://github.com/icbi-lab/immunedeconv)]. Markers related to immune multicellular structures (e.g., tertiary lymphoid structures) or immune functions (e.g., immunosuppression) were obtained from published signatures (33, 34).

Statistical Analyses

Analysis of efficacy endpoints was performed using the IRC assessment of response according to RECIST v1.1. According to parameters, statistical data are expressed in the form of frequencies and percentages (qualitative variables), mean and standard deviation, median and interquartile range (quantitative variables), and survival curve estimates calculated with the Kaplan–Meier method. In translational analyses, statistical tests are mentioned in the legends of the figures and included Fisher exact test, Kruskal–Wallis rank sum test, and Pearson Chi-squared test. Each primary and secondary evaluation criterion is reported with a CI of 95% unless otherwise mentioned. The Cox model was used to assess the HR when comparing subgroups for PFS and OS. Data have been analyzed with the SAS (SAS Inc.) and R (https://www.R-project.org/) software packages.

Concerning the statistical methodology for comparison of Pan-Cancer and COAD/READ groups (Fig. 1E and F), we used one-way ordinary ANOVA tests allowing multiple comparison of MSS POLE pathogenic category with other categories, corrected for multiplicity using Dunnet test. Analyses were performed on MCPcounter, EPIC, or XCELL output for each parameter of interest using GraphPad software version 9. The level of significance displayed in the figures is as follows: ns, nonsignificant, >0.05; *, ≥0.05 and >0.01; **, ≤0.01 and >0.001; ***, ≤0.001 and >0.0001; ****, ≤0.0001. Similar statistical methodology was used for comparisons for Figs. 1D, 3B, and 4D and E.

Tumor IHC

An IHC study using antibodies to CD3, CD8, and PD-L1 was performed on one patient both in pretreatment biopsies and a surgical specimen (35). For PD-L1, slides were incubated with the clone QR1 (Diagomics) on unstained tissue sections (4 μm) using the Leica Bond III platform automated stainer according to the manufacturers' recommendations. Positive PD-L1 expression was defined as any membranous staining in either tumor cells or in infiltrating inflammatory cells. The percentage of tumor cells demonstrating membranous PD-L1 staining was also scored in 5% increments. T cells in the tumor-associated immune infiltrates were assessed by semiquantitative estimation of CD3-positive (CD3: Thermo Scientific, clone SP7, 1:300 dilution) and CD8-positive (CD8: DAKO, clone C8/144B, 1:30

dilution) cell densities. They were scored as follows: 0, no positive cells; 1, scattered positive cells; 2, moderate number of positive cells; and 3, abundant occurrence of positive cells. In each tumor, the density of T-cell infiltration was examined at the invasive front (cells localized in stroma adjacent to the invasive tumor margin) and in the intratumoral compartment.

MSK Cohort of Patients with Colorectal Cancer Exposed to Immune-Checkpoint Inhibitors

The characteristics of the MSK colorectal cancer cohort have been presented before. In brief, clinical and genetic data from patients followed at MSKCC with colorectal cancer who underwent testing from 2015 through 2020 with the next-generation sequencing targeted MSK-IMPACT panel of somatic mutations were obtained from an internal database (26–28). Patients who underwent MSK-IMPACT testing and had metastatic or unresectable and locally advanced ($n = 140$) colon or rectal adenocarcinoma and who received at least one immune-checkpoint inhibitor between April 11, 2014, and December 2, 2019, were identified. Clinical–demographic data and cancer characteristics (histology, primary tumor location, staging) as well as prior treatment details were extracted from the electronic medical record and verified by licensed physicians (S.B. Maron and B.H. Diplas). MMRd status and POLE status were determined as reported in the Methods. The study was approved by the MSKCC IRB (2020-013).

Data Availability

A part of the analyses that support the findings of this study are based upon data generated by the TCGA Research Network (https://www.cancer.gov/tcga) and are openly available at https://portal.gdc.cancer.gov/projects.

Other reported data from the Acsé POLE clinical trials and MSK cohort of patients with colorectal cancer exposed to immune-checkpoint inhibitors are available by the corresponding authors upon reasonable request. The data are not publicly available due to information that could compromise the privacy of research participants.

Authors' Disclosures

B. Rousseau reports nonfinancial support from FoundationOne, grants and personal fees from Neophore, other support from Bristol Myers Squibb and MSKCC, and grants from Swim Across America and the Nuovo-Soldati Foundation during the conduct of the study; personal fees from Bayer, Roche, Servier, and Gilead outside the submitted work; and a patent for methods and composition for cancer immunotherapy issued to MSKCC. R. Cohen reports personal fees and nonfinancial support from Bristol Myers Squibb and MSD Oncology during the conduct of the study, as well as personal fees from Amgen and Pierre Fabre, nonfinancial support from Mylan Medical, and grants from Servier Institute outside the submitted work. V. Simmet reports personal fees from Lilly, Servier, and Sanofi outside the submitted work. P. Augereau reports personal fees and nonfinancial support from AstraZeneca, Pfizer, and GlaxoSmithKline, nonfinancial support from Novartis, and personal fees from Covis outside the submitted work. D. Malka reports grants from Bristol Myers Squibb during the conduct of the study, as well as personal fees and nonfinancial support from Amgen, Bayer, Bristol Myers Squibb, Merck Serono, Merck, Pierre Fabre, Roche, Sanofi, and Servier, and personal fees from Incyte, Viatris, and AstraZeneca outside the submitted work. A. Hollebecque reports grants from Bristol Myers Squibb during the conduct of the study, as well as grants and personal fees from Incyte, grants from AstraZeneca, Bristol Myers Squibb, Boehringer Ingelheim, Janssen Cilag, Novartis, Pfizer, Roche, and Sanofi, and personal fees from Amgen, Bayer, Debiopharm, QED Therapeutics, Eisai, and Lilly outside the submitted work. D. Pouessel reports grants and personal fees from AstraZeneca and Bristol Myers Squibb, grants from Incyte, Roche, Janssen Oncology, and Seagen, grants, personal fees, and nonfinancial support from MSD, personal fees and nonfinancial support from Pfizer, and personal fees from Merck and Ipsen outside the submitted work. C. Gomez-Roca reports other support from Institut National du Cancer during the conduct of the study; grants and personal fees from Roche/Genentech and Bristol Myers Squibb, personal fees from Eisai and Foundation Medicine, and nonfinancial support from MSD, Pierre Fabre, and Macomics outside the submitted work; and is an ESMO Officer. M. Guillet reports personal fees from Bayer and Servier, and nonfinancial support from Sanofi, Roche, and Amgen outside the submitted work. J.-J. Grob reports personal fees from Bristol Myers Squibb, Merck, Novartis, Roche, Philogen, Sanofi, Pierre Fabre, and Amgen outside the submitted work. C. de la Fouchardiere reports personal fees from Ipsen and Incyte, grants and nonfinancial support from Pierre Fabre Oncologie, and personal fees and nonfinancial support from MSD, Servier, Amgen, Bayer, Eisai, Lilly, Daiichi Sankyo, Merck, and Roche outside the submitted work. F. Rolland reports personal fees from Bristol Myers Squibb and MSD during the conduct of the study. S. Hiret reports personal fees and other support from Takeda, Bristol Myers Squibb, Roche, and AstraZeneca outside the submitted work. E. Saada-Bouzid reports personal fees from Bristol Myers Squibb, MSD, and Merck Serono outside the submitted work. O. Bouche reports personal fees from Merck KGaA, Roche, Bayer, AstraZeneca, Grunenthal, MSD, Amgen, Servier, and Pierre Fabre outside the submitted work. T. Andre reports personal fees from Bristol Myers Squibb, AstraZeneca, Amgen, Astellas Pharma, Gritstone Oncology, GlaxoSmithKline, HallioDx, Kaleido Biosciences, MSD, Pierre Fabre, Roche, Seagen, Servier, and Transgene outside the submitted work. S. Oudard reports grants and personal fees from Bristol Myers Squibb, Pfizer, Novartis, Sanofi, and Bayer, and personal fees from Merck, Janssen, and Astellas outside the submitted work. C. Tournigand reports nonfinancial support and other support from Bristol Myers Squibb during the conduct of the study, as well as nonfinancial support and other support from MSD, Sanofi, and Bayer outside the submitted work. J.-C. Soria reports other support from Gritstone Bio, Relay Therapeutics, Amgen, and AstraZeneca outside the submitted work. S. Champiat reports personal fees from Amgen, AstraZeneca, Bristol Myers Squibb, Eisai, Janssen, MSD, Novartis, and Roche, other support (as principal investigator of clinical trials) from AbbVie, Amgen, Cytovation, Eisai, Imcheck Therapeutics, Molecular Partners Ag, MSD, Ose Pharma, Pierre Fabre, Sanofi Aventis, Sotio A.S, and Transgene, other support (as an advisory board member) from Alderaan Biotechnology, Amgen, AstraZeneca, Avacta, Ellipses Pharma, Oncovita, Seagen, and UltraHuman, and other support (travel and congress) from AstraZeneca, MSD, Ose Pharma, Roche, and Sotio outside the submitted work; as part of the Drug Development Department (DITEP) for Gustave Roussy is/has been the principal/subinvestigator of clinical trials for AbbVie, Adaptimmune, Adlai Nortye USA Inc., Aduro Biotech, Agios Pharmaceuticals, Amgen, Argen-X Bvba, Arno Therapeutics, Astex Pharmaceuticals, AstraZeneca Ab, Aveo, Basilea Pharmaceutica International Ltd., Bayer Healthcare Ag, Bbb Technologies Bv, Beigene, BicycleTx Ltd., Bioalliance Pharma, Blueprint Medicines, Boehringer Ingelheim, Boston Pharmaceuticals, Bristol Myers Squibb, Ca, Celgene Corporation, Chugai Pharmaceutical, Cullinan-Apollo, CureVac, Daiichi Sankyo, Debiopharm, Eisai, Eisai Limited, Eli Lilly, Exelixis, Faron Pharmaceuticals Ltd., Forma Tharapeutics, Gamamabs, Genentech, GlaxoSmithKline, H3 Biomedicine, Hoffmann La Roche Ag, Imcheck Therapeutics, Innate Pharma, Institut De Recherche Pierre Fabre, Iris Servier, Iteos Belgium SA, Janssen Cilag, Janssen Research Foundation, Kura Oncology, Kyowa Kirin Pharm. Dev, Lilly France, Loxo Oncology, Lytix Biopharma As, MedImmune, Menarini Ricerche, Merck Sharp & Dohme-Chibret, Merus, Molecular Partners Ag, Nanobiotix, Nektar Therapeutics, Novartis Pharma, Octimet Oncology Nv, Oncoethix, Oncopeptides, Onyx Therapeutics, Orion Pharma, Oryzon Genomics, Ose Pharma, Pfizer, Pharma Mar, Pierre Fabre

Médicament, Plexxikon, Roche, Sanofi Aventis, Seattle Genetics, Sotio A.S, Syros Pharmaceuticals, Taiho Pharma, Tesaro, Turning Point Therapeutics, and Xencor; research grants from AstraZeneca, Bristol Myers Squibb, Boehringer Ingelheim, GlaxoSmithKline, INCa, Janssen Cilag, Merck, Novartis, Pfizer, Roche, and Sanofi; and nonfinancial support (drug supplied) from AstraZeneca, Bayer, Bristol Myers Squibb, Boehringer Ingelheim, GlaxoSmithKline, MedImmune, Merck, NH TherAGuiX, Pfizer, and Roche. M.F. Lamendola-Essel reports personal fees from Rockefeller University outside the submitted work. S.B. Maron reports personal fees from Natera, Bicara, Novartis, Daiichi Sankyo, and Basilea, and nonfinancial support from Bayer, Guardant Health, and Genentech outside the submitted work, as well as prior Calithera stock ownership. G. Argiles reports personal fees from Gadeta BV and other support from Amgen outside the submitted work. N.H. Segal reports personal fees from AstraZeneca, GlaxoSmithKline, Novartis, ABL Bio, Revitope, Amgen, Boehringer Ingelheim, and PsiOxus, grants and personal fees from Roche/Genentech, Immunocore, and PureTech Ventures, and grants from Pfizer, Merck, Bristol Myers Squibb, and Regeneron outside the submitted work. A. Cercek reports personal fees from Bayer, Merck, GlaxoSmithKline, Seagen, and Janssen, and grants from Seagen, GlaxoSmithKline, and RGenix outside the submitted work. L.A. Diaz Jr is a member of the board of directors for Jounce Therapeutics; is a compensated consultant for PetDx, Innovatus CP, Se'er, Delfi, Kinnate, and Neophore; is an uncompensated consultant for Merck but has received clinical trial support from Merck; is an inventor of multiple licensed patents related to technology for circulating tumor DNA analyses and mismatch repair deficiency for diagnosis and therapy from Johns Hopkins University (some of these licenses and relationships are associated with equity or royalty payments directly to Johns Hopkins and L.A. Diaz Jr); and holds equity in Jounce Therapeutics, PetDx, Se'er, Delfi, Kinnate, and Neophore. L.A. Diaz Jr divested his equity in Personal Genome Diagnostics to LabCorp in February 2022 and divested his equity in Thrive Earlier Detection to Exact Biosciences in January 2021. His spouse holds equity in Amgen. The terms of all these arrangements are being managed by Johns Hopkins and Memorial Sloan Kettering in accordance with their conflict of interest policies. P. Saintigny reports grants from Illumina, HTG Molecular Diagnostics, AstraZeneca, Roche, Bristol Myers Squibb Foundation, Novartis, and Inivata, and personal fees from Archer and Roche Molecular Diagnostics during the conduct of the study, as well as grants from Omicure outside the submitted work. A. Marabelle reports grants from Ligue contre le Cancer and Bristol Myers Squibb, and nonfinancial support from Institut National du Cancer during the conduct of the study; grants, personal fees, nonfinancial support, and other support from Bristol Myers Squibb, MSD, and Roche/Genentech, personal fees and other support from Pfizer/Merck Serono, other support from AstraZeneca, and grants, personal fees, and other support from Sanofi outside the submitted work; and was the lead investigator of the KN-158 trial that contributed to the approval of pembrolizumab for MSI- and TMB-high tumors. No disclosures were reported by the other authors.

One of the Editors-in-Chief is an author on this article. In keeping with the AACR's editorial policy, the peer review of this submission was managed by a member of *Cancer Discovery*'s Board of Scientific Editors, who rendered the final decision concerning acceptability.

Authors' Contributions

B. Rousseau: Conceptualization, formal analysis, supervision, investigation, methodology, writing–original draft, writing–review and editing. **I. Bieche:** Conceptualization, formal analysis, supervision, investigation, methodology, writing–original draft, writing–review and editing. **E. Pasmant:** Conceptualization, formal analysis, supervision, investigation, methodology, writing–original draft, writing–review and editing. **N. Hamzaoui:** Conceptualization, data curation, formal analysis, supervision, investigation, writing–review and editing. **N. Leulliot:** Formal analysis, investigation, visualization, writing–review and editing. **L. Michon:** Data curation, software, investigation, methodology. **A. de Reynies:** Data curation, software, investigation, visualization, methodology. **V. Attignon:** Resources, data curation. **M.B. Foote:** Formal analysis, investigation, writing–review and editing. **J. Masliah-Planchon:** Formal analysis, investigation, writing–review and editing. **M. Svrcek:** Formal analysis, investigation, visualization, writing–review and editing. **R. Cohen:** Investigation, writing–review and editing. **V. Simmet:** Investigation, writing–review and editing. **P. Augereau:** Investigation, writing–review and editing. **D. Malka:** Investigation, writing–review and editing. **A. Hollebecque:** Investigation, writing–review and editing. **D. Pouessel:** Investigation, writing–review and editing. **C. Gomez-Roca:** Investigation, writing–review and editing. **R. Guimbaud:** Investigation. **A. Bruyas:** Investigation, writing–review and editing. **M. Guillet:** Investigation, writing–review and editing. **J.-J. Grob:** Investigation. **M. Duluc:** Investigation. **S. Cousin:** Investigation. **C. de la Fouchardiere:** Investigation. **A. Flechon:** Investigation. **F. Rolland:** Investigation. **S. Hiret:** Investigation. **E. Saada-Bouzid:** Investigation. **O. Bouche:** Investigation. **T. Andre:** Investigation, writing–review and editing. **D. Pannier:** Investigation. **F. El Hajbi:** Investigation. **S. Oudard:** Investigation. **C. Tournigand:** Investigation. **J.-C. Soria:** Investigation. **S. Champiat:** Conceptualization. **D.G. Gerber:** Data curation, investigation. **D. Stephens:** Data curation, investigation. **M.F. Lamendola-Essel:** Resources, project administration, writing–review and editing. **S.B. Maron:** Data curation, investigation, writing–review and editing. **B.H. Diplas:** Data curation, investigation. **G. Argiles:** Investigation, writing–review and editing. **A.R. Krishnan:** Data curation, investigation. **S. Tabone-Eglinger:** Resources, data curation. **A. Ferrari:** Resources, data curation, software. **N.H. Segal:** Investigation, writing–review and editing. **A. Cercek:** Investigation. **N. Hoog-Labouret:** Supervision. **F. Legrand:** Supervision. **C. Simon:** Resources, supervision, project administration. **A. Lamrani-Ghaouti:** Data curation, supervision, project administration. **L.A. Diaz Jr:** Supervision, investigation, writing–review and editing. **P. Saintigny:** Conceptualization, resources, formal analysis, supervision, investigation, methodology, writing–review and editing. **S. Chevret:** Conceptualization, formal analysis, supervision, methodology, writing–original draft, writing–review and editing. **A. Marabelle:** Conceptualization, supervision, investigation, methodology, writing–original draft, writing–review and editing.

Acknowledgments

The Acsé Nivolumab trial is sponsored by the French network of comprehensive cancer centers (Unicancer) and the Institut National du Cancer (INCa). The funding of the trial has been supported by Bristol Myers Squibb, the Ligue contre le Cancer (www.ligue-cancer.net), and l'INCa. The supply of nivolumab was kindly provided by Bristol Myers Squibb. Blood PBMCs and tumor FFPE blocks were prospectively collected, stored, and prepared for analysis by the Léon Bérard Cancer Center (Centre de Ressources Biologiques du Centre Léon Bérard, #BB-0033-00050, Lyon, France). The sequencing of tumors (WES and RNA-seq) was part of the ancillary analysis program of Acsé Nivolumab (Acsé Cible) funded by a research grant from the Ligue contre le Cancer. B. Rousseau thanks the Nuovo-Soldati and Swim Across America foundations for salary support. This work was funded in part by the Marie-Josée and Henry R. Kravis Center for Molecular Oncology and NCI Cancer Center Core Grant P30-CA008748. We gratefully acknowledge the members of the Molecular Diagnostics Service in the Department of Pathology of MSKCC. Also, we thank Mr. Daniel Couch, the genomic platform personnel who screened for patients harboring *POLE* mutations, all the study coordinators, the nurses, and the patients and their families who have actively participated in the POLE cohort of the Acsé Nivolumab trial. This work was supported by Bristol Myers Squibb, Unicancer, the Ligue contre le Cancer, and INCa. M.B. Foote is funded by an NIH

T32-CA009512 and an ASCO Young Investigator Award. This work was also supported by funding from the Integrated Cancer Research Site LYriCAN (INCa-DGOS-Inserm_12563) and PIA Institut Convergence Francois Rabelais PLAsCAN (PLASCAN, 17-CONV-0002).

Received May 26, 2021; revised March 9, 2022; accepted April 4, 2022; published first April 10, 2022.

REFERENCES

1. Rayner E, van Gool IC, Palles C, Kearsey SE, Bosse T, Tomlinson I, et al. A panoply of errors: polymerase proofreading domain mutations in cancer. Nat Rev Cancer 2016;16:71–81.
2. Campbell BB, Light N, Fabrizio D, Zatzman M, Fuligni F, de Borja R, et al. Comprehensive analysis of hypermutation in human cancer. Cell 2017;171:1042–56.
3. Chalmers ZR, Connelly CF, Fabrizio D, Gay L, Ali SM, Ennis R, et al. Analysis of 100,000 human cancer genomes reveals the landscape of tumor mutational burden. Genome Medicine 2017;9:34.
4. Alexandrov LB, Kim J, Haradhvala NJ, Huang MN, Tian Ng AW, Wu Y, et al. The repertoire of mutational signatures in human cancer. Nature 2020;578:94–101.
5. Hodel KP, Sun MJS, Ungerleider N, Park VS, Williams LG, Bauer DL, et al. POLE mutation spectra are shaped by the mutant allele identity, its abundance, and mismatch repair status. Mol Cell 2020;78:1166–77.
6. Samstein RM, Lee C-H, Shoushtari AN, Hellmann MD, Shen R, Janjigian YY, et al. Tumor mutational load predicts survival after immunotherapy across multiple cancer types. Nat Genet 2019;51:202–6.
7. Marabelle A, Fakih M, Lopez J, Shah M, Shapira-Frommer R, Nakagawa K, et al. Association of tumour mutational burden with outcomes in patients with advanced solid tumours treated with pembrolizumab: prospective biomarker analysis of the multicohort, open-label, phase 2 KEYNOTE-158 study. Lancet Oncol 2020;21:1353–65.
8. Rousseau B, Foote MB, Maron SB, Diplas BH, Lu S, Argilés G, et al. The spectrum of benefit from checkpoint blockade in hypermutated tumors. N Engl J Med 2021;384:1168–70.
9. Briggs S, Tomlinson I. Germline and somatic polymerase ε and δ mutations define a new class of hypermutated colorectal and endometrial cancers. J Pathol 2013;230:148–53.
10. Church DN, Stelloo E, Nout RA, Valtcheva N, Depreeuw J, ter Haar N, et al. Prognostic significance of POLE proofreading mutations in endometrial cancer. J Natl Cancer Inst 2015;107:402.
11. Hamzaoui N, Alarcon F, Leulliot N, Guimbaud R, Buecher B, Colas C, et al. Genetic, structural, and functional characterization of POLE polymerase proofreading variants allows cancer risk prediction. Genet Med 2020;22:1533–41.
12. Wang F, Zhao Q, Xu R-H. Evaluation of POLE/POLD1 variants as potential biomarkers for immune checkpoint inhibitor treatment outcomes-reply. JAMA Oncol 2020;6:590.
13. Rousseau B, Vidal J, Diaz LA. Evaluation of POLE/POLD1 variants as potential biomarkers for immune checkpoint inhibitor treatment outcomes. JAMA Oncol 2020;6:589–90.
14. Palles C, Cazier JB, Howarth KM, Domingo E, Jones AM, Broderick P, et al. Germline mutations affecting the proofreading domains of POLE and POLD1 predispose to colorectal adenomas and carcinomas. Nat Genet 2013;45:136–44.
15. Le DT, Uram JN, Wang H, Bartlett BR, Kemberling H, Eyring AD, et al. PD-1 blockade in tumors with mismatch-repair deficiency. N Engl J Med 2015;372:2509–20.
16. Le DT, Durham JN, Smith KN, Wang H, Bartlett BR, Aulakh LK, et al. Mismatch repair deficiency predicts response of solid tumors to PD-1 blockade. Science 2017;357:409–13.
17. Garmezy B, Gheeya J, Lin HY, Huang Y, Kim T, Jiang X, et al. Clinical and molecular characterization of POLE mutations as predictive biomarkers of response to immune checkpoint inhibitors in advanced cancers. JCO Precis Oncol 2022;6:e2100267.
18. Litchfield K, Reading JL, Puttick C, Thakkar K, Abbosh C, Bentham R, et al. Meta-analysis of tumor- and T cell-intrinsic mechanisms of sensitization to checkpoint inhibition. Cell 2021;184:596–614.
19. Chung J, Maruvka YE, Sudhaman S, Kelly J, Haradhvala NJ, Bianchi V, et al. DNA polymerase and mismatch repair exert distinct microsatellite instability signatures in normal and malignant human cells. Cancer Discov 2020;11:1176–91.
20. Berry SM, Broglio KR, Groshen S, Berry DA. Bayesian hierarchical modeling of patient subpopulations: efficient designs of phase II oncology clinical trials. Clin Trials 2013;10:720–34.
21. Trippa L, Lee EQ, Wen PY, Batchelor TT, Cloughesy T, Parmigiani G, et al. Bayesian adaptive randomized trial design for patients with recurrent glioblastoma. J Clin Oncol 2012;30:3258–63.
22. Mandrekar SJ, Sargent DJ. Clinical trial designs for predictive biomarker validation: theoretical considerations and practical challenges. J Clin Oncol 2009;27:4027–34.
23. Richards S, Aziz N, Bale S, Bick D, Das S, Gastier-Foster J, et al. Standards and guidelines for the interpretation of sequence variants: a joint consensus recommendation of the American College of Medical Genetics and Genomics and the Association for Molecular Pathology. Genet Med 2015;17:405–24.
24. Niu B, Ye K, Zhang Q, Lu C, Xie M, McLellan MD, et al. MSIsensor: microsatellite instability detection using paired tumor-normal sequence data. Bioinformatics 2014;30:1015–6.
25. Salipante SJ, Scroggins SM, Hampel HL, Turner EH, Pritchard CC. Microsatellite instability detection by next generation sequencing. Clin Chem 2014;60:1192–9.
26. Gao J, Aksoy BA, Dogrusoz U, Dresdner G, Gross B, Sumer SO, et al. Integrative analysis of complex cancer genomics and clinical profiles using the cBioPortal. Sci Signal 2013;6:pl1.
27. Cerami E, Gao J, Dogrusoz U, Gross BE, Sumer SO, Aksoy BA, et al. The cBio cancer genomics portal: an open platform for exploring multidimensional cancer genomics data. Cancer Discov 2012;2:401–4.
28. Cheng DT, Mitchell TN, Zehir A, Shah RH, Benayed R, Syed A, et al. Memorial Sloan Kettering-Integrated Mutation Profiling of Actionable Cancer Targets (MSK-IMPACT): a hybridization capture-based next-generation sequencing clinical assay for solid tumor molecular oncology. J Mol Diagn 2015;17:251–64.
29. Wagner GP, Kin K, Lynch VJ. Measurement of mRNA abundance using RNA-seq data: RPKM measure is inconsistent among samples. Theory Biosci 2012;131:281–5.
30. Becht E, Giraldo NA, Lacroix L, Buttard B, Elarouci N, Petitprez F, et al. Estimating the population abundance of tissue-infiltrating immune and stromal cell populations using gene expression. Genome Biol 2016;17:218.
31. Aran D, Hu Z, Butte AJ. xCell: digitally portraying the tissue cellular heterogeneity landscape. Genome Biol 2017;18:220.
32. Racle J, Gfeller D. EPIC: a tool to estimate the proportions of different cell types from bulk gene expression data. Methods Mol Biol 2020;2120:233–48.
33. Becht E, de Reyniès A, Giraldo NA, Pilati C, Buttard B, Lacroix L, et al. Immune and stromal classification of colorectal cancer is associated with molecular subtypes and relevant for precision immunotherapy. Clin Cancer Res 2016;22:4057–66.
34. Petitprez F, de Reyniès A, Keung EZ, Chen TW, Sun CM, Calderaro J, et al. B cells are associated with survival and immunotherapy response in sarcoma. Nature 2020;577:556–60.
35. Dahlin AM, Henriksson ML, Van Guelpen B, Stenling R, Oberg A, Rutegård J, et al. Colorectal cancer prognosis depends on T-cell infiltration and molecular characteristics of the tumor. Mod Pathol 2011;24:671–82.